

Review

Research Progress on Novel Electrochemical Descaling Technology for Enhanced Hardness Ion Removal

Liangtian Wang [†], Jie Zhou [†], Yuexin Chang and Hao Xu ^{*ID}

Department of Environmental Science Engineering, Xi'an Jiaotong University, Xi'an 710049, China; 13751525121@163.com (L.W.); zhoujie5355@163.com (J.Z.); cyx1815@163.com (Y.C.)

* Correspondence: xuhao@xjtu.edu.cn

[†] These authors contributed equally to this work.

Abstract: In recent years, electrochemical descaling technology has gained widespread attention due to its environmental friendliness and ease of operation. However, its single-pass removal efficiency could be higher, severely limiting its practical application. To overcome the limitations of traditional electrochemical descaling processes, this paper first focuses on the separation efficiency of H⁺ and OH⁻ in the scale removal process based on numerous recent research papers. It mainly emphasizes how innovative cathode design can enhance the efficiency and stability of electrochemical descaling. Furthermore, this paper explores the coupling of electrochemical processes with different water treatment technologies, such as the combination of electrodeposition with electrocoagulation, filtration crystallization, microfiltration, and electrodialysis, and how these methods synergistically enhance descaling effects. Additionally, this paper discusses potential future directions for electrochemical descaling technology, including innovations in scale expansion, material updates, process optimization, system integration, and automation. Finally, this paper analyzes the practical challenges of electrochemical descaling technology, such as cost, energy consumption, equipment durability, and environmental impact, and proposes solutions. The implementation of these strategies is expected to promote the commercialization of electrochemical descaling technology, making it more aligned with the sustainability requirements of industry and the environment.

Keywords: electrochemical descaling; H⁺-OH⁻ separation; cathode design; coupled processes



Citation: Wang, L.; Zhou, J.; Chang, Y.; Xu, H. Research Progress on Novel Electrochemical Descaling Technology for Enhanced Hardness Ion Removal. *Water* **2024**, *16*, 886. <https://doi.org/10.3390/w16060886>

Academic Editor: Andrea G. Capodaglio

Received: 14 February 2024

Revised: 5 March 2024

Accepted: 15 March 2024

Published: 19 March 2024



Copyright: © 2024 by the authors. Licensee MDPI, Basel, Switzerland. This article is an open access article distributed under the terms and conditions of the Creative Commons Attribution (CC BY) license (<https://creativecommons.org/licenses/by/4.0/>).

1. Introduction

China's total industrial water consumption accounts for approximately 20% of the national water usage, second only to agricultural water usage. Among them, the usage of industrial circulating cooling water (CCW) is substantial, with a wide range of applications in various industrial processes such as petrochemical, metal smelting, and power generation [1–3], constituting around 80% of the total industrial water usage [4–6]. The CCW system effectively manages heat in industrial processes by recycling water as a cooling medium. In this system, CCW first flows through heat-generating equipment, such as heat exchangers or reactors, to absorb the generated heat. Subsequently, the heated water is transported to cooling towers or other cooling devices and cooled through contact with air or radiators [7,8]. Open-loop circulating cooling water systems are widely used in industrial production. However, due to their direct exposure to the atmosphere, as heat is dissipated through convective air cooling, water continuously evaporates from the CCW, increasing salt content and hardness ion concentration in the water [9,10]. Additionally, impurity ions such as carbonate (HCO₃⁻), phosphate (PO₄³⁻), and nitrate (NO₃⁻) enter the CCW along with rainwater or suspended particles in the air, causing an increase in hardness and alkalinity [11]. As the hardness and alkalinity ions encounter heat exchanger surfaces during the circulation of cooling water, precipitation quickly occurs due to the higher temperatures, ultimately leading to scaling on the surfaces of heat exchangers and pipes [12–16].

Scale formation in circulating cooling systems poses several hazards, including (1) scale, being a poor conductor, can impede heat transfer during the circulation process, indirectly affecting production efficiency and, in severe cases, may lead to hazardous events like explosions; (2) scale can reduce the flow area in pipes, increasing fluid resistance and thus energy consumption; (3) excessive scale deposition necessitates shutdowns for cleaning, reducing equipment operational time and efficiency [17–22]. Hence, addressing scale formation in CCW is urgent, not only for average industrial production and economic benefits but also for conserving water resources and ensuring industrial safety [23,24].

Industrial scale prevention and removal methods in CCW systems include dosing, ultrasonic, ion exchange softening, reverse osmosis, and electrochemical descaling [25]. Dosing, the most widely used method in industrial CCW, is time-efficient, simple to operate, and generally effective. It typically involves either scale inhibitors, which complex with calcium (Ca^{2+}) and magnesium (Mg^{2+}) ions in water to prevent their deposition on heat exchanger surfaces and disperse existing scale [26–28], or lime softening, which reacts lime with calcium bicarbonate in solution to precipitate scale [29,30]. However, scale inhibitors cannot remove hardness ions, only delay their precipitation, and organophosphorus inhibitors may lead to P contamination, further causing pollution [31–33]. Lime softening has high chemical costs and generates excessive sludge, requiring further treatment [34]. Ultrasonic antiscalant works by changing the physical structure of the medium (e.g., causing cracks) due to mechanical vibrations caused by ultrasonic waves, leading to scale loosening and detachment from heat exchanger walls [35]. However, ultrasonic equipment is costly and prolonged use may cause equipment to loosen. In ion exchange, commonly used sodium ion exchange resins swap Na^+ for Ca^{2+} , reducing Ca^{2+} concentration to inhibit scale formation. This method requires periodic regeneration or replacement of the ion exchange resin and post-treatment to avoid secondary pollution due to increased Na^+ concentration in water [36]. Reverse osmosis applies pressure to one side of a membrane solution to overcome osmotic pressure, causing the solvent to permeate from the high-pressure side to the low-pressure side. At the same time, solutes are retained, effectively separating ions [37,38]. Although highly effective at scale removal, over the long-term operation, concentrated scaling ions can deposit on the membrane surface, clogging pores, reducing descaling efficiency, and increasing energy consumption [39,40].

Electrochemical descaling is an innovative, eco-friendly process that offers no need for additional chemicals, pollution-free operation, easy regulation, simple process structure, and the potential for automation [41,42]. During electrochemical descaling, water decomposition near the anode produces oxygen and an acidic environment, while hydrogen and an alkaline environment are created near the cathode. In this alkaline environment, hardness ions like Ca^{2+} and Mg^{2+} and HCO_3^- chemically react to form insoluble calcium carbonate (CaCO_3) and magnesium carbonate (MgCO_3) [43]. Additionally, hydroxide ions (OH^-) produced by water electrolysis combine with Mg^{2+} to form magnesium hydroxide ($\text{Mg}(\text{OH})_2$), which can then be removed from the water [18]. Furthermore, oxidation reactions at the anode generate strong oxidants like H_2O_2 , O_3 , and ClO^- , which are effective for sterilization, algae control, and COD removal [44,45].

Despite the advantages of electrochemical descaling technology, traditional methods face several challenges that require improvement: (1) the reaction of cathodically generated OH^- with anodically produced H^+ leads to a low utilization rate of OH^- and, thus, inefficient descaling; (2) the cathode not only produces OH^- but also provides sites for deposition, making traditional electrochemical, which is dominated by heterogeneous precipitation dependent on a highly effective cathode area; (3) single electrochemical descaling, primarily electrodeposition, often fails to meet effluent standards in a single treatment, necessitating integration with other technologies. To address these issues, scholars have conducted extensive research in recent years. This review summarizes recent papers on H^+ - OH^- separation technology, cathode design, and coupled electrochemical descaling processes. It concludes by discussing the commercial challenges of electrochemical descaling technology and proposes future research directions and opportunities.

2. H⁺-OH⁻ Separation

OH⁻ plays a crucial role in the electrochemical descaling process. When an electric current passes through the electrodes in a water treatment system, the cathode undergoes reduction of water molecules, generating hydrogen gas (H₂) and OH⁻. These OH⁻ increase the pH near the cathode area, creating an alkaline environment. Under such conditions, OH⁻ reacts with HCO₃⁻ to form CO₃²⁻, precipitating with Ca²⁺ as calcium carbonate (CaCO₃) [46]. A high concentration of OH⁻ also reacts with Mg²⁺ to form Mg(OH)₂ precipitates [47,48], which can be subsequently removed to reduce scale formation and accumulation. The required pH for efficient precipitation of Ca²⁺ and Mg²⁺ is above 9 and 10, respectively [49]. Therefore, the generation of OH⁻ and the subsequent precipitation reactions are central to electrochemical descaling [50].

It is well known that oxidation and reduction of water molecules at the anode and cathode during electrochemical reactions generates large amounts of H⁺ and OH⁻, respectively. However, under the influence of the electric field, H⁺ and OH⁻ migrate towards the cathode and anode, leading to a neutralization reaction that results in low utilization of OH⁻ in the descaling process, and, consequently, a low hardness removal rate [51]. Traditional electrochemical descaling efficiency is only about 15% to 25% [52]. Effective separation of H⁺ and OH⁻ is an efficient way to enhance hardness removal rates. Different H⁺-OH⁻ separation methods in electrochemical descaling were compared as shown in Table 1.

Table 1. Comparison of different H⁺-OH⁻ separation methods in electrochemical descaling.

Separation Method		Water Hardness	pH	Hardness Removal Rate	Hardness Precipitation	Energy Consumption	References
Ion exchange membrane (IEMs)	Cation exchange membrane (CEMs)	188 mg/L Ca ²⁺	9.8	75~86%	-	7.0~10.1 kWh/kg CaCO ₃	[44]
	Anion exchange membrane (AEMs)	500 mg/L CaCO ₃	-	-	64~85 g/h/m ²	9~12 kWh/kg CaCO ₃	[53]
	Bipolar membrane	16 mM Ca ²⁺	-	-	630 g/h/m ²	1.2 kWh/kg CaCO ₃	[54]
	Polytetrafluoroethylene membrane (PTFE)	400 mg/L CaCO ₃	11.5	-	348.8 g/h/m ² CaCO ₃	1.88 kWh/kg CaCO ₃	[55]
	Confined crystallization membrane (CCM)	500 mg/L CaCO ₃	-	-	60.26 g/h/m ² CaCO ₃	12 kWh/kg CaCO ₃	[56]
	Extraction of boundary layer	500 mg/L CaCO ₃	11.7	92%	-	4.6 kWh/kg CaCO ₃	[57]
Bubbles and water flow	Nylon net	500 mg/L CaCO ₃	11.5	91.5%	-	12.6 kWh/kg CaCO ₃	[58]
	Water flow	400 mg/L CaCO ₃	10.6	-	151.2 g/h/m ² CaCO ₃	16.8 kWh/kg CaCO ₃	[59]

2.1. Membrane-Based H⁺-OH⁻ Separation

2.1.1. Ion Exchange Membrane (IEMs)

In electrochemical descaling, membrane materials play a versatile and crucial role, mainly isolating the anode and cathode and providing ion-selective permeability [60]. The most used membranes are IEMs, which are categorized into cation exchange membranes (CEMs) and anion exchange membranes (AEMs). These membranes are characterized by their selective permeability to specific types of ions. CEMs allow only cations (such as Ca²⁺, Mg²⁺, etc.) to pass through, while AEMs permit the passage of anions (such as CO₃²⁻, SO₄²⁻, etc.) [35]. Beyond allowing the passage of specific ions, IEMs also prevent the mixing of other substances, such as the H₂ and OH⁻ generated at the cathode area, from mixing with the O₂ and H⁺ produced at the anode area, thereby enhancing the safety and descaling efficiency of the system.

Clauwaert et al. [44] partitioned the electrolytic cell into two compartments using cation and AEMs for electrochemical descaling experiments. When using CEMs, the pH in the cathode chamber rises rapidly due to the impermeability of OH⁻ through the membrane, which aids in the removal of hardness. During this process, the average removal rates for Ca²⁺ and Mg²⁺ hardness were 75–86% and 7–21%, respectively, with an energy consumption of 7.0–10.1 kWh/kg CaCO₃. When using AEMs, Ca²⁺ and Mg²⁺ migrate towards the cathode and accumulate on the surface of the membrane facing the anode side; meanwhile, OH⁻ and HCO₃⁻ pass through the AEM and move towards the anode. On the other side of the membrane, they react with the accumulated Ca²⁺ and Mg²⁺ to form CaCO₃ and Mg(OH)₂. During this process, the removal rates for Ca²⁺ and Mg²⁺ hardness were 73–78% and 40–44%, respectively, at an energy consumption of 5.8–7.5 kWh/kg CaCO₃. Both IEMs enabled reagent-free water softening at relatively low energy costs in the electrochemical descaling process. Jin et al. [53] proposed an IEM electrochemical precipitation descaling process (Figure 1a), which used only an AEM to remove hardness from CCW through electrochemical precipitation occurring at the surface of the AEM. This IEM electrodeposition descaling process showed good operational stability, maintaining high descaling performance with a steady and consistent operation. The precipitation rate and energy consumption were 64–85 g/h/m² and 9–12 kWh/kg CaCO₃, respectively. Parameters such as Ca²⁺ concentration, Mg²⁺ concentration, alkalinity, conductivity, etc., significantly influenced the process’s precipitation rate and hardness removal efficiency.

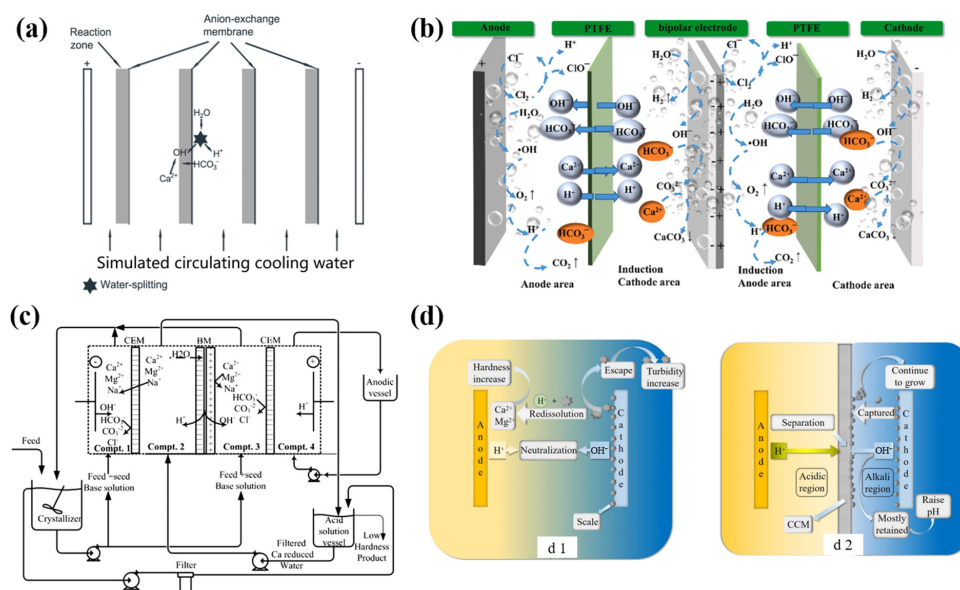


Figure 1. Reaction mechanism diagrams: (a) electrochemical descaling with IEMs, (b) bipolar membrane electrochemical descaling, (c) high-efficiency bypass bipolar electrolytic descaling system, (d) The flow of scale and acid-base ions in two electrochemical systems: (d1) electrochemical descaling system without CCM, (d2) electrochemical descaling system with CCM.

Electrochemical descaling performance can be enhanced by combining bipolar membranes with membrane-based electrolytic cells to improve descaling capability. A bipolar membrane is a composite membrane consisting of two ion exchange layers joined together either physically or chemically. One of the layers is an AEM of fixed positive charge that permits transport of anions. The other layer is a CEM of fixed negative charges that permits transport of cations. Integration of bipolar membranes with ion exchange membranes enables more effective production of the alkalinity required for CaCO₃ removal. Zaslavski et al. [54] placed a bipolar membrane between two CEMs, with the reaction mechanism shown in Figure 1b. The OH⁻ produced in compartments 1 and 3 by the cathode reaction and by the bipolar membrane is utilized for CaCO₃ removal. The feed solution, dosed with OH⁻ generated in the two compartments, is recycled through the crystallizer where CaCO₃

is precipitated on seeds. In experiments treating brackish water containing 16 mM Ca^{2+} , the process achieved a CaCO_3 precipitation rate of approximately 630 g/h/m² at a current density of 10 mA/cm², with an energy consumption of 1.2 kWh/kg CaCO_3 . In contrast, a system using only CEMs for electrochemical descaling showed a CaCO_3 precipitation rate of just 520 g/h/m², with a higher energy consumption of 1.4 kWh/kg CaCO_3 . Integrating bipolar membranes can significantly enhance the current efficiency and reduce energy consumption in electrochemical membrane-based descaling processes. Compared to traditional electrodeposition techniques, ion membrane electrodeposition descaling technology improves descaling performance and dramatically reduces equipment costs, offering broad application prospects.

2.1.2. Polytetrafluoroethylene (PTFE) Membrane

In membrane-based electrolytic cells, the neutralization reaction of H^+ and OH^- is slower than undivided electrolytic cells; hence, preventing the neutralization of H^+ and OH^- does not solely rely on the selectivity of the IEMs. Additionally, under the influence of an electric field, Ca^{2+} and Mg^{2+} migrate towards the cathode, while OH^- and HCO_3^- move towards the anode. The accumulation of these ions near the IEM leads to the formation of scale on the membrane surface, resulting in clogging and increased energy consumption.

Therefore, a non-selective, porous, and robust separation material can serve as an alternative separator in electrolytic cells. Liu et al. [55] found that when using a hydrophilic PTFE membrane as the separator, ions such as Ca^{2+} , Mg^{2+} , H^+ , HCO_3^- , CO_3^{2-} , and OH^- could easily pass through the PTFE membrane, maintaining electrical neutrality in the anode and cathode chambers. As the current density increased from 20 A/m² to 100 A/m², the scale precipitation rate increased from 97.5 to 348.8 g/h/m² CaCO_3 , and the specific energy consumption rose from 0.68 to 1.88 kWh/kg CaCO_3 . Liu et al. [47] developed an efficient electrochemical descaling system to remove Ca^{2+} hardness from brackish water (Figure 1c), utilizing a bipolar electrode to enhance OH^- production and PTFE membrane as the separation material between anode and cathode. At a current density of 20 mA/cm², the optimal Ca^{2+} hardness removal efficiencies at the induction cathode and final effluent were 85% and 57%, respectively, with a CaCO_3 precipitation rate of 2.2 kWh/kg CaCO_3 . The best Ca^{2+} hardness removal was achieved with a molar ratio of Ca^{2+} to HCO_3^- of 1:1.2.

2.1.3. Confined Crystallization Membrane (CCM)

Although PTFE membranes exhibit good chemical stability and excellent temperature resistance [61], challenges such as manufacturing difficulties, high membrane resistance, and a propensity for bubble adhesion persist. Li et al. [56] developed a novel CCM electrochemical descaling process to address the issues associated with IEMs and PTFE membranes. CCM takes advantage of the high alkalinity environment in the cathode area to induce precipitation of hardness ions near the diaphragm, thereby accelerating the removal of hardness from the CCW (Figure 1d). Experiments demonstrated that the CCM could mitigate the impact of concentration polarization on mass transfer, creating a high pH and low water flow environment conducive for scale precipitation. Compared to traditional electrochemical descaling, this process improved hardness removal efficiency by at least 4.09% at a current density of 2 mA/cm² and increased current efficiency by 10.2% at 8 mA/cm². Even at a high circulating inflow rate of 9 L/h, this method maintained a high descaling rate, with a scaling deposition rate of 60.26 g/h/m² CaCO_3 , which was 32.97 g/h/m² higher than that of traditional electrochemical descaling processes.

The above results indicate that it is relatively easy to implement electrochemical descaling strategies by inhibiting the neutralization reaction of H^+ and OH^- to increase the pH in the cathode chamber. Although the electrochemical descaling process based on IEM/polytetrafluoroethylene membrane/confined crystallization membrane can achieve high descaling efficiency, its practical industrial application is limited due to the complex membrane fabrication process, high cost, and sensitivity to high oxidants, organic sub-

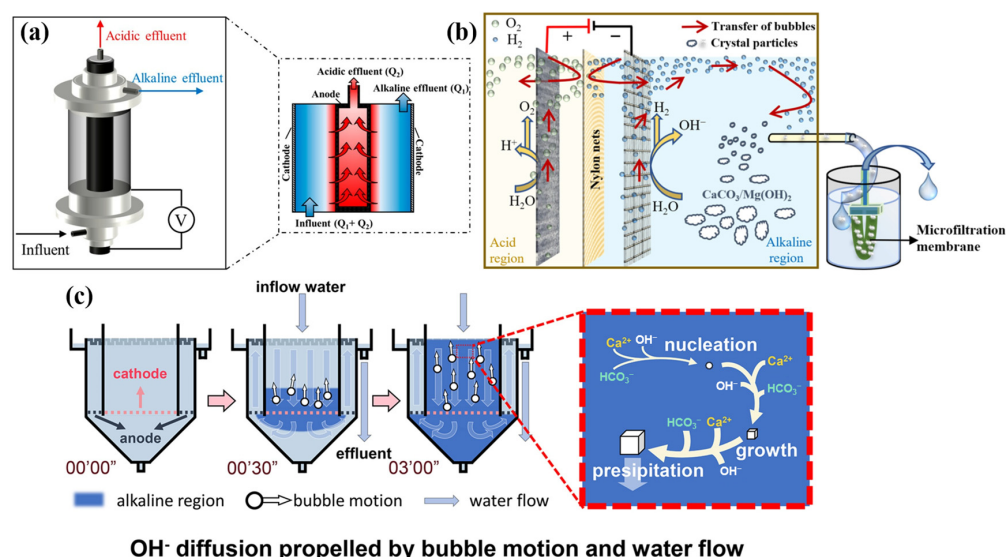
stances, pollution, and scaling in actual water bodies. These limitations are destined to weaken the dominant position of membrane-based electrolytic cells in descaling processes.

2.2. In Situ Membrane-Free H⁺-OH⁻ Separation

Analysis from the previous section indicates that while using membranes in electrochemical descaling processes can improve efficiency, the complexity of membrane fabrication and the associated high production costs, along with the impediment to charge migration and increased energy consumption during electrochemical reactions, are considerable drawbacks. Furthermore, the scale can easily clog the pores of the membrane [54,62]. Therefore, exploring the in situ membrane-free separation of H⁺ and OH⁻ is a valuable endeavor.

2.2.1. Extraction of Boundary Layer Solution

It is well known that in water electrolysis, the H⁺ produced at the anode and OH⁻ produced at the cathode are initially confined within the boundary layer of the electrode surface (less than 100 μm thick). They migrate towards the cathode and anode under the electric field's action and are eventually neutralized and consumed in the bulk solution [51]. Inspired by this phenomenon, Ba et al. [57] proposed using a tubular porous titanium filter as the anode; by extracting the anode boundary layer solution at an appropriate rate, the diffusion of H⁺ generated at the anode into the bulk solution can be prevented (Figure 2a). Consequently, the OH⁻ generated at the cathode can increase the pH of the bulk solution, facilitating the removal of hardness ions from the solution. Experiments have shown that with increasing current density and inflow rate, the H⁺-OH⁻ separation performance declined, mainly due to enhanced electromigration and turbulence at the anode surface. At an inflow rate of 500 mL/min and current density of 6–22 mA/cm², the separation efficiency for H⁺ and OH⁻ in acidic and alkaline effluents was 10~72% and 16~94%, respectively, while the Ca²⁺ hardness removal efficiency was 42~92%, with an energy consumption of 1.2~4.6 kWh/kg of CaCO₃. This process exhibits superior H⁺-OH⁻ separation performance compared to membrane separation systems. Due to the extraction of the boundary layer solution rich in H⁺ from the tubular anode in this process, the anode is always in a high acidic environment. Prolonged operation under such conditions can shorten the lifespan of the anode and increase operational costs.



OH⁻ diffusion propelled by bubble motion and water flow
Figure 2. (a) Continuous electrolytic cell structures with anode boundary layer extraction, (b) schematic of the electrochemical descaling process with nylon net separation, (c) diagram illustrating the mechanism of electrochemical descaling promoted by bubble motion and water flow diffusion.

2.2.2. Bubbles and Water Flow

The random diffusion of H₂ bubbles generated from water electrolysis can cause flow disturbances near the cathode, creating turbulence [63,64], and water flow has also been found to accelerate ion diffusion [65,66]. Utilizing these characteristics, it is deduced that bubble diffusion and water flow can be harnessed to expedite the diffusion of OH⁻ from the cathode surface and effectively separate OH⁻ and H⁺. Kang et al. [58] utilized a sandwich structure of mesh cathode, nylon net, and mesh anode to divide the electrolytic cell into anode and cathode chambers (Figure 2b). During continuous operation, OH⁻ was rapidly pushed from the cathode surface to the cathode chamber by the motion of water flow and H₂ bubbles produced by cathode electrolysis. The average diameters of H₂ and O₂ bubbles during electrolysis are approximately 3.5 μm and 53.4 μm, respectively [67], and a 400-mesh nylon net with a pore size of 25.0 μm was used in this study, allowing for the passage of H₂ bubbles while potentially obstructing the transmission of O₂ bubbles. The unidirectional transport of H₂ bubbles may isolated some of the H⁺ generated at the anode, thus forming an extensive alkaline area in the cathode chamber that enhances the homogeneous precipitation of hardness ions. After running with seven layers of 400-mesh nylon nets for 30 min, the pH in the cathode chamber can reach 11.5, whereas with a proton exchange membrane under the same conditions, the pH was 11.0. Compared to the latter, the nylon net offered better H⁺-OH⁻ separation, higher quality, and lower cost. At a current density of 12 mA/cm² and a hydraulic retention time of 20 min, the total hardness removal rate reached 91.5%, with an energy consumption of 12.6 kWh/kg CaCO₃. In order to restore electrical neutrality within the reactor, the nylon mesh structure in the system cannot prevent the migration of OH⁻ from the cathode chamber to the anode chamber, as well as the migration of hardness ions from the anode chamber to the cathode chamber. Prolonged operation under these conditions can result in fouling and blockage of the nylon mesh.

Mao et al. [59] developed a reactor modeled after vertical flow sedimentation tanks, featuring an upper hollow cylindrical body and a lower inverted hollow conical body. The mesh cathode, central tube, and mesh anode were placed concentrically from the center outwards. Water flowed in from the central tube, first passing through the mesh circular cathode, then through the mesh annular anode, and overflowed from the top of the reactor (Figure 2c). During operation, H₂ bubbles generated by water electrolysis moved upwards while the inflowing water moved downwards. Within 3 min, the average pH in the central tube reached 10.6. At a current density of 80 A/m² and an inflow rate of 6 L/h, the declining efficiency was 151.2 g/h/m² CaCO₃, with a current efficiency of 57%. During this process, the homogeneous nucleation of CaCO₃ within the central tube was crucial in hardness removal. The reactor has a simple design, which makes it easy to replicate and implement. However, due to the parallel placement of the anode and cathode in this reactor, the voltage in the reactor was high, resulting in a high energy consumption during the electrochemical descaling process. When the current density is 80 mA/cm², the voltage can reach up to 30 V. Additionally, the vertical flow of water through the porous anode will inevitably lead to scaling and blockage with prolonged operation, further increasing the voltage. The novel electrochemical descaling reactors have achieved efficient descaling without the use of membrane materials. However, they are still in the laboratory-scale stage, and the specific electrode configuration and arrangement pose challenges for scaling up.

The analysis indicates that membrane materials can efficiently separate H⁺ and OH⁻, enhancing electrochemical descaling efficiency. However, high costs and poor fouling resistance limit their large-scale industrial application. Recent developments in novel membrane-free electrochemical descaling reactors have prevented H⁺-OH⁻ neutralization and improved descaling efficiency without using membranes but introduced complexities and higher energy consumption, with their practical application efficacy yet to be fully validated.

3. Cathode Design

During the electrochemical descaling process, cathodic electrolysis of water produces H₂ and OH⁻. In the solution, HCO₃⁻, Ca²⁺, and Mg²⁺ react with OH⁻ on the cathode

surface to form CaCO_3 and $\text{Mg}(\text{OH})_2$ precipitates [68]. As the reaction progresses, the scale layer gradually covers the cathode surface [69]. This reduces the working area of the cathode, impedes the electrolysis reaction and mass transfer processes, and increases electrode resistance, decreasing in hardness removal efficiency and higher energy consumption [70,71]. Regular cathode cleaning is required to maintain efficiency, which further increases operational costs [45]. In electrochemical devices, in order to achieve good treatment performance, it is usually necessary to design the cathode to obtain a large working electrode surface area, thereby improving the efficiency of electrochemical descaling. The comparison of different cathodes electrochemical descaling is shown in Table 2.

Table 2. Comparison of different cathodes in electrochemical descaling.

Cathode		Water Hardness	Hardness Removal Rate	Hardness Precipitation	Energy Consumption	References
Two-dimensional cathode	Multi-layer stainless steel	350 mg/L CaCO_3	-	29.16 g/h/m ²	6 kWh/kg CaCO_3	[72]
	Multiple cathodes	350 mg/L CaCO_3	-	71.1 g/h/m ² ,	3.17 kWh/kg CaCO_3	[73]
Three-dimensional cathode	Stainless steel wire	2400 mg/L CaCO_3	45%	-	-	[43]
	Stainless steel ball fluidized bed	64 mg/L Ca^{2+} ; 7.5 mg/L Mg^{2+}	-	-	0.375 kWh/m ³	[74]
Combined cathode	Stainless steel-carbon felt	1.8 mmol/L Ca^{2+} ; 1.8 mmol/L Mg^{2+}	Ca^{2+} : 91%; Mg^{2+} : 38.6%,	-	Ca^{2+} : 0.68 kWh/mol; Mg^{2+} : 1.68 kWh/mol	[75]
	Graphite-polymer composite	7.845 mmol/L Ca^{2+}	90%	-	45.9 kWh/kg CaCO_3	[76]

3.1. Two-Dimensional Cathode

Different cathode materials significantly influence scale deposition in the electrochemical descaling process. Mirror-finish stainless steel cathodes exhibit the highest descaling performance, followed by regular stainless steel, nickel plates, brushed stainless steel, and titanium plates [77]. Additionally, due to their larger specific surface area and rougher texture, mesh cathodes have a higher rate of hardness deposition than flat cathodes [50]. Many researchers are focusing on increasing the effective cathode area. Luan et al. [72] studied the electrochemical descaling efficiency of multi-layer stainless steel mesh cathodes of various mesh sizes (Figure 3a). Results indicated that the synergistic effect of the outer and inner layers of stainless steel mesh enhanced the descaling efficiency of the coupled cathodes. The shielding effect results in significant differences in current density and potential between the layers, leading to preferential scale deposition on the outer cathode layer [78]. Additionally, the inner layer cathode experienced minimal interference from H^+ in the hydrogen evolution reaction, resulting in a higher pH in the inner solution, which favored further removal of hardness ions. At a current density of 18.3 A/m² and an inflow rate of 500 mL/h, the descaling rate was 29.16 g/h/m², with an energy consumption of 6 kWh/kg CaCO_3 .

Yu et al. [73] designed a multi-stage reactor with a “Z”-shaped flow by staggered arrangement of electrodes, which increased the contact area between the solution and electrodes while reducing internal dead zones, enhancing the efficiency of hardness removal (Figure 3b). In comparison with conventional electrochemical reactors, the multi-stage reactor not only has less back mixing, short circuit, and dead zone, but also has high volumetric efficiency, leading to better treatment performance. This was mainly because the multi-stage reactor showed typical plug flow regime. In general, the single-stage reactor was considered as the completely mixed reactor because of the bubble turbulence effect, while the multi-stage reactor consisting of a series of single cells could work as a manner of the plug flow. The initial hardness concentration of the plug flow reactor was much higher than that of the completely mixed reactor, which enhanced the precipitation

reactions and the mass transfer, improving the softening efficiency significantly. In their experiments, with four DSA anodes and five stainless steel cathodes alternately fixed, a precipitation rate of 71.1 g/h/m² was achieved at a current density of 40 A/m² and a hydraulic retention time of 8.2 min. The current efficiency was 37.6%, with an energy consumption of only 3.17 kWh/kg CaCO₃, and the descaling efficiency remained stable over long-term operation. In traditional two-dimensional cathode systems, due to the low utilization of OH⁻, the current efficiency for hardness removal is usually below 20% when the energy consumption exceeds 9.0 kWh/kg CaCO₃, and the hardness content is within the range of 300–600 mg/L [79].

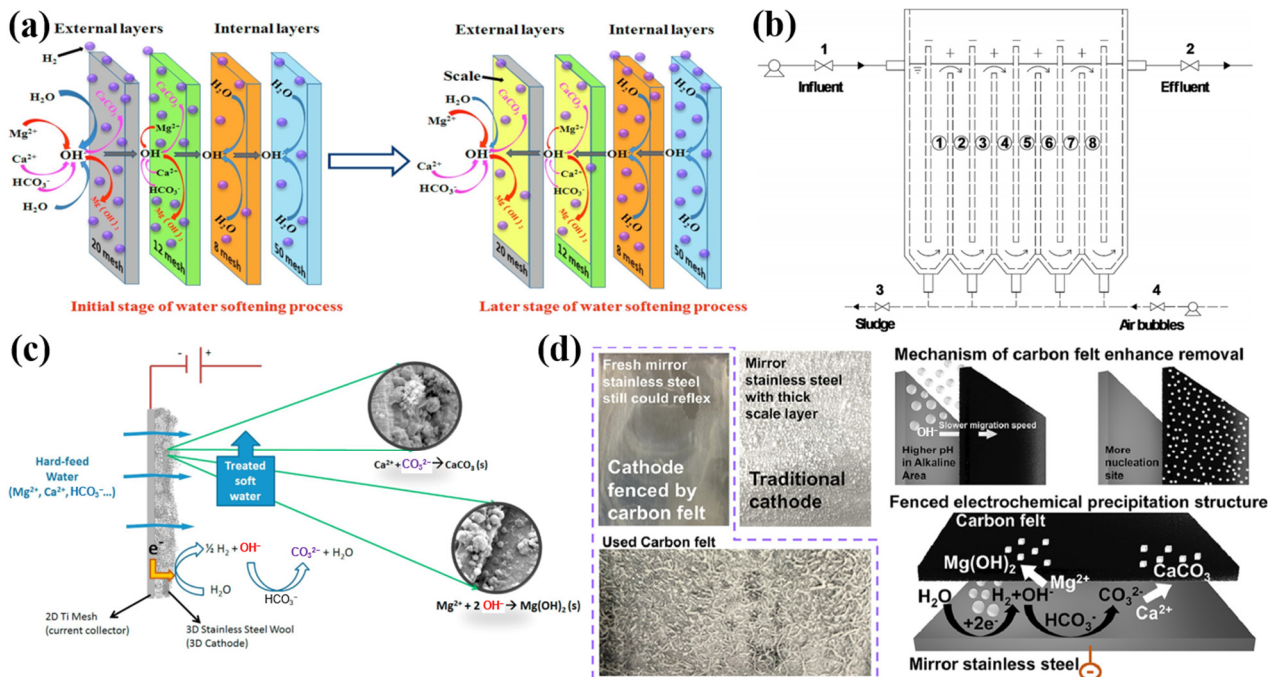


Figure 3. (a) Schematic of the coupled cathode working principle, (b) schematic of a multi-stage reactor for electrochemical descaling, (c) diagram of the electrochemical descaling reaction mechanism for a three-dimensional cathode, (d) diagram of the electrochemical descaling reaction mechanism for a gate-type cathode.

3.2. Three-Dimensional Cathode

Compared to two-dimensional cathodes, three-dimensional cathodes, due to their larger specific surface area, offer more deposition sites for heterogeneous precipitation of CaCO₃ [76], thus exhibiting higher hardness removal efficiency. Furthermore, the diffusion rate of OH⁻ into the bulk solution is slowed down, which improves the utilization of OH⁻ to a certain extent. The results indicate that the three-dimensional cathode system can suppress the neutralization reaction between H⁺ and OH⁻, resulting in higher current efficiency compared to the two-dimensional cathode system. Hence, Sanjuán et al. [43] utilized stainless steel wool as a cathode to study its electrochemical descaling effect (Figure 3c). The results showed that at a current density of 100 A/m² and an inflow rate of 12 L/h, the three-dimensional cathode achieved a hardness removal rate of up to 40%, approximately 20% higher than that of a conventional titanium mesh cathode. However, long-term experiments indicated that while three-dimensional cathodes performed better than two-dimensional cathodes within the first 30 h, they experienced more significant clogging over time and structural collapse within the cathode, leading to a rapid decline in descaling performance.

Marchesiello et al. [74] introduced a fluidized bed between the two electrodes, filled with 1 mm diameter 316 stainless steel balls, which significantly improved the descaling capacity of the system. The fluidized stainless steel balls serve as both the anode and

cathode, allowing for simultaneous electrochemical reactions and thorough treatment of the solution in the entire vessel. In accelerated scale deposition tests, a reduction of nearly 90% in CaCO_3 precipitation was observed at a current density of 50 mA/cm^2 . A total of 80 L of solution was treated within 2 h, consuming only 0.03 kWh (or 0.375 kWh/m^3) of energy. However, due to the limited increase in cathode surface area, scaling on the cathode surface can still occur during long-term operation, leading to hindered OH^- production, reduced hardness removal, and increased energy consumption. Overall, the deposition of scale on the cathode surface is an unavoidable phenomenon in the process of hardness removal, which hampers descaling efforts. Although fluidized beds show promising descaling performance, they are often prone to the influence of water matrix, hydraulic retention time, and seed characteristics [80,81].

3.3. Combined Cathode

Despite the increase in effective cathode surface area and the enhanced descaling efficiency of reactors from previous studies, the issue of scale deposition on cathodes still poses a challenge for maintaining long-term, high-efficiency hardness removal [62]. Therefore, Yang et al. [75] devised a novel gate-type cathode for hardness removal (Figure 3d). This cathode consisted of a mirror-finished stainless steel plate covered with a carbon felt layer, which utilized the porous structure of the carbon felt to slow down the diffusion of OH^- generated by cathodic water electrolysis into the bulk solution, while also providing numerous sites for scale deposition. This internal alkaline environment within the carbon felt promoted the removal of hardness ions. The experimental results showed that at a current density of 40 A/m^2 , the removal efficiencies for Ca^{2+} and Mg^{2+} were increased by 12.8% and 46.1%, respectively, compared to those using only stainless steel cathodes, with energy consumptions as low as 0.68 kWh/mol for Ca^{2+} and 1.68 kWh/mol for Mg^{2+} . Moreover, it was found that most of the Ca^{2+} and Mg^{2+} hardness removal occurred on the carbon felt, facilitating cathode replacement and continuous operation of the process. However, the treatment system only transferred the scaling from the cathode surface to other materials and cannot maintain a high descaling efficiency in the long term.

In order to remove the insoluble scale generated on the cathode during the electrochemical descaling process and improve the descaling efficiency, Muddemann et al. [76] developed an electrochemical reactor with a graphite–polymer composite (GPC) as the cathode and boron-doped diamond as the anode. The experiment revealed that the most suitable GPC cathode was a 0.5 mm thick polypropylene-based composite material, which exhibited chemical stability and low resistivity ($5.06 \pm 1.80 \text{ m}\Omega \text{ cm}$). The results showed that at a current density of 0.5 kA/cm^2 , the incoming water hardness was reduced by more than 72% and 90% in the mixed and separated electrolyte modes, respectively. During long-term treatment exceeding 120 h, only a small amount of scale deposited on the GPC cathode, possibly due to the formation of a very thin solid layer on the cathode surface, leading to a balanced cycle of scale deposition and detachment, thereby preventing further scale formation on the cathode. Although this process prevents cathodic scaling and exhibits high descaling efficiency, the preparation of the cathode is complex and costly, and there are still many challenges to overcome in transitioning from the laboratory to practical applications.

4. Coupling Process

Due to the limited removal of hardness ions in solutions by standalone electrochemical descaling technology, which mainly induces electrochemical precipitation, coupled processes leverage the complementary nature of different technologies to enhance removal efficiency, reduce operational costs, broaden application scope, and improve produced water quality. Consequently, extensive research has been made in electrochemical descaling coupled processes [25,82]. The comparison of different coupling processes electrochemical descaling is shown in Table 3.

Table 3. Comparison of coupling processes in electrochemical descaling.

Coupling Process		Water Hardness	Hardness Removal Rate	Hardness Precipitation	Energy Consumption	References
Electrodeposition–electrocoagulation	Electrodeposition–electrocoagulation synergy	300 mg/L CaCO ₃	65%	-	-	[83]
	Membrane polarization catalytic electrocoagulation	350 mg/L CaCO ₃	-	318.9 g/h/m ²	3.8 kWh/kg CaCO ₃	[84]
Electrodeposition–filtration crystallization	Conventional electrodeposition filtration	300 mg/L CaCO ₃	15.6~33.4%	-	-	[85]
	Reverse polarity descaling–filtration crystallization	300 mg/L CaCO ₃	25.5~27.3%	-	-	[52]
Electrodeposition–microfiltration	Electrochemical accelerated precipitation decaling–microfiltration	400 mg/L CaCO ₃	-	348.8 g/h/m ² CaCO ₃	1.88 kWh/kg CaCO ₃	[55]
	Electrolysis–microfiltration–ion exchange	400 mg/L CaCO ₃	90%	-	1.9 kWh/Kg CaCO ₃	[76]
Electrodeposition–Electrodialysis		6400 mg/L CaCO ₃	Ca ²⁺ : 57%; Mg ²⁺ : 61%,	5.8–15.9 M/h/m ²	-	[86]

4.1. Electrodeposition–Electrocoagulation

Electrocoagulation is a promising method for removing hardness from water [87]. The flocs formed during the electrocoagulation process offer ample precipitation zones for hardness removal, overcoming the limitations of the cathodic area on electrochemical descaling. Zhi et al. [83] proposed a method that synergized electrochemical precipitation with electrocoagulation to remove hardness from CCW. They discovered that the lower the initial hardness concentration at different current densities, the better the synergistic effect. Moreover, this synergistic effect was only observed when electrocoagulation was performed prior to electrochemical precipitation. The experimental results indicated that the optimal synergy was achieved under the following conditions: an electrocoagulation current density of 20 A/m², an electrochemical precipitation current density of 250 A/m², an inflow rate of 120 mL/min, a pH of 7.2, a water temperature of 60 °C, and a treatment time of 130 min, resulting in a hardness removal efficiency of 65%. However, the slow hydrolysis reaction severely limits the formation of flocs, thereby inhibiting hardness removal, and the dissolved Al³⁺ can cause secondary pollution. Yu et al. [84] proposed to significantly improve the efficiency of electrocoagulation for hardness removal by introducing membrane polarization to catalyze H₂O dissociation. Membrane polarization induced water dissociation will generate abundant OH⁻, which beneficial for the floc production process, substantially enhancing the co-precipitation efficiency for hardness removal. Better still, the promoted formation of floc will simultaneously minimize the dissolved Al³⁺, circumventing secondary pollution. When the current density is 100 A/m², the flow rate is 40 L/h, pH is 8.1, and the incoming water hardness is 350 mg/L, the removal of hardness was achieved through various pathways: ion exchange, electrodeposition, electrocoagulation, induced ion exchange membrane, and other pathways remove 3.4%, 16.8%, 20%, 54.4%, and 5.4% of the hardness, respectively. Electrodeposition relies solely on cathodic precipitation reactions, while the abundant flocs generated during electrocoagulation can provide sufficient nucleation sites for homogeneous precipitation of hardness ions, allowing for hardness removal to overcome the limitations of the cathode region.

The membrane-enhanced electrocoagulation process can achieve an ultra-high hardness removal rate of 318.9 g/h/m² and an ultra-low energy consumption of 3.8 kWh/kg CaCO₃, greatly outperforming other conventional hardness removal processes. However, in the electrocoagulation process, the anode is continuously consumed, and a large amount of floc sludge is generated, which undoubtedly increases operational costs.

4.2. Electrodeposition–Filtration Crystallization

During electrochemical descaling, not all scale precipitates adhere to the cathode; some disperse within the reactor, potentially causing re-dissolution and reducing descaling efficiency. Therefore, Guo et al. [85] introduced an electrochemical–filtration crystallization coupled process (Figure 4a). This system effectively intercepted scaling particles in the effluent and provided numerous deposition sites for homogeneous precipitation of CaCO₃, further purifying the CCW. Experiments showed that after continuous operation for 360 min under conditions of 300 mg/L hardness, a 1:1 alkalinity ratio, a peristaltic pump speed of 10 rpm, a current density of 6 mA/cm², with DSA electrodes as the anode, a titanium mesh as the cathode, and synthetic zeolite as filler, the hardness removal rate of the coupled process ranged from 15.6 to 33.4%, significantly exceeding the 9.46 to 18.07% achieved by the standalone electrochemical descaling process. Zhou et al. [52] used plate titanium sub-oxide electrodes as both anode and cathode in electrochemical descaling, leveraging the oxidative and reductive properties of the electrodes and combining them with polarity reversal for continuous descaling. However, some detached scale was found to exit with the effluent, affecting water quality. Hence, a filtration crystallization system using synthetic zeolite as filler was coupled after the electrochemical process (Figure 4b). Results indicated that the optimal descaling performance, stable between 17% and 20%, was achieved at a current density of 8 mA/cm² and flow rate of 2.7 L/h. Coupling with the filtration crystallization system increased hardness removal rates from 25.5% to 27.3%. However, in a filtration crystallization system, the porous materials used for trapping and adsorbing a large quantity of scale particles can become clogged after prolonged operation. Therefore, the focus should be on developing suitable methods for regeneration to address this issue.

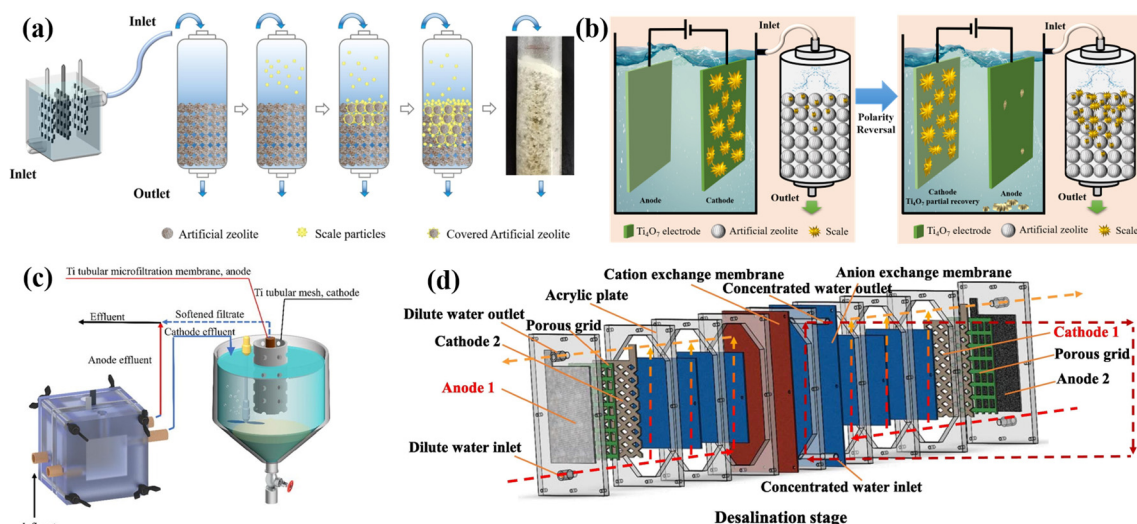


Figure 4. (a) Schematic of the electrochemical descaling–filter crystallization coupled process, (b) mechanism diagram of the electrochemical polarity reversal descaling–filter crystallization coupled process, (c) diagram of the electrochemical accelerated precipitation–microfiltration coupled process apparatus, (d) schematic of the membrane deposition electro dialysis process apparatus.

4.3. Electrodeposition–Microfiltration

During accelerated nucleation of scale particles, homogeneous precipitation in the bulk solution forms small scale particles with diameters <0.15 mm. Therefore, microfiltration,

with its small footprint, ease to operation, and manageability, is an effective method for solid–liquid separation, offering extensive surface area for CaCO_3 nucleation and growth, which enhances crystallization and descaling efficiency. Liu et al. [55] developed an electrochemical accelerated precipitation softening–microfiltration (EAPS-MF) system for the removal of Ca^{2+} hardness from solutions (Figure 4c). In this process, an electrolytic cell is divided by a polytetrafluoroethylene membrane, with alkaline effluent directly entering the crystallizer to form CaCO_3 crystals, which are then intercepted by a titanium pipe microfilter. Within this system, as the current density increases from 20 A/m^2 to 100 A/m^2 , the precipitation rate of CaCO_3 increases from 975 g/h/m^2 to 348.8 g/h/m^2 , with energy consumption rising from $0.68 \text{ kWh/kg CaCO}_3$ to $1.88 \text{ kWh/kg CaCO}_3$. Ba et al. [42] developed an electrolytic cell that extracts H^+ from the anode boundary layer to enhance hardness removal efficiency and combined it with microfiltration and ion exchange for scale removal. In this system, the effluent from the electrolytic cell was intercepted by a porous tubular titanium microfilter in the crystallizer and further treated with ion exchange resin. Experimental results showed that the filter cake enhanced hardness removal during microfiltration. This is because the high flow velocity and large surface area inside the narrow pores of the filter cake increase the random collision probability between ions, potentially leading to heterogenous crystallization within the filter cake. At a current density of 10 mA/cm^2 , the total hardness can be reduced from 400 mg/L to 40 mg/L , achieving a removal efficiency of 90% with an energy consumption of $1.9 \text{ kWh/kg CaCO}_3$. However, the use of microfiltration membranes in the microfiltration process still cannot avoid the inherent defects of the membrane material.

4.4. Electrodeposition–Electrodialysis

The electrodialysis process can also enhance the removal of hardness ions from the solution, utilizing the potential difference as the driving force [88–90]. To address the limited ion selectivity in removing other ions of traditional electrochemical descaling technologies in removing hardness ions from water, Yu et al. [86] developed a membrane deposition electrodialysis process, which combined conventional electrochemical precipitation with electrodialysis for ion removal (Figure 4d). Experiments demonstrated that, compared to traditional electrodialysis methods, membrane deposition electrodialysis not only utilized electrophoresis to remove common ions but also employed membrane deposition for efficient hardness ion removal, aiding in achieving zero discharge. At a current density of 200 A/m^2 and an inflow rate of 4 L/h , the process achieved 57% and 61% removal efficiency for Ca^{2+} and Mg^{2+} ions, respectively. The hardness removal rate of the membrane deposition electrodialysis process can reach $5.8\text{--}15.9 \text{ M/h/m}^2$, 1.5–26.5 times higher than traditional processes. However, coupling electrodialysis can further increase operational costs and add complexity to the process, requiring careful consideration in practical applications.

5. Summary and Outlook

This review thoroughly investigates the critical mechanisms of electrochemical scaling removal techniques and the research efforts made in recent years to enhance the efficiency of these techniques. Firstly, the importance of separating H^+ and OH^- and the role of cathode design in improving scale removal performance were analyzed. While the use of membrane materials can suppress neutralization reactions, the defects in membrane materials severely affect their widespread application. Although some novel membrane-free reactors and cathode designs can achieve efficient scale removal, there is still a lack of investigation on their large-scale, long-term operation, and economic feasibility. Subsequently, this paper also summarized the coupling of electrochemical descaling technology with other water treatment methods and discussed the potential enhancement of scale removal effectiveness through such coupling. While coupling with other processes can improve scale removal efficiency, operational costs and process complexity also increase, necessitating a reasonable trade-off based on actual water quality and operational conditions. Despite some challenges,

this review also highlights the significance of electrochemical descaling technologies in water treatment due to their environmentally friendly nature and efficiency.

Future developments in electrochemical descaling technology will focus on several key innovations: (1) Scaling up: although numerous novel reactors boast high descaling efficiency, their complex structures and electrode arrangements hinder large-scale application, necessitating further investigation into their practical use and industrial viability. (2) Material innovation: in electrochemical descaling technology, both cathodes and membrane materials face issues of scaling and clogging during long-term operation, making it essential to develop electrodes and membranes that are more efficient, easier to clean, longer-lasting, and cost-effective. (3) Process optimization: utilizing advanced simulation tools for optimizing electrochemical descaling processes, ensuring optimal operating conditions for minimal energy consumption, and maximized descaling efficiency. (4) Coupling technologies: electrochemical descaling coupling technologies primarily focus on two aspects: improving the reactor's descaling efficiency and expediting the following homogeneous precipitation, suggesting the exploration of novel processes from these two perspectives. (5) Automation and intelligence: implementing IoT, big data, and artificial intelligence (AI) technologies to achieve intelligent monitoring and automated management of electrochemical descaling systems, improving adaptability and ease of operation. (6) Sustainability research: conducting more in-depth research into the environmental impacts of electrochemical descaling technology, assessing its sustainability throughout its lifecycle, and exploring its potential in a circular economy. (7) Standardization and scaling: establishing clear industry standards and operating procedures to allow for the broader industrial and municipal application of electrochemical descaling technology on a larger scale.

Challenges faced by electrochemical descaling technology in practical applications include system cost, operational complexity, durability, and environmental issues. Strategies to address these challenges may include the following: (1) Cost reduction: lowering initial investment and operational costs by optimizing the design of novel membrane-free electrochemical reactors and developing cathodes that facilitate the deposition and detachment of scale. (2) Simplification of operation: developing user-friendly interfaces and automated control strategies to reduce reliance on skilled technicians. (3) Enhanced durability: investigating and utilizing new materials to improve system components' corrosion resistance and mechanical stability. (4) Minimizing environmental impact: assessing and mitigating the environmental footprint of the electrochemical descaling process, such as the recycling and reusing of electrode materials. With these strategies, electrochemical descaling technology is expected to see wide application and continued development in the field of water treatment.

Author Contributions: Conceptualization, L.W. and H.X.; methodology, H.X.; software, Y.C.; validation, L.W. and J.Z.; formal analysis, L.W. and H.X.; investigation, H.X.; data curation, Y.C.; writing—original draft preparation, L.W. and J.Z.; writing—review and editing, H.X.; visualization, Y.C.; All authors have read and agreed to the published version of the manuscript.

Funding: This research was funded by National Natural Science Foundation of China, grant number 52270078.

Data Availability Statement: No new data were created or analyzed in this study. Data sharing is not applicable to this article.

Conflicts of Interest: The authors declare no conflicts of interest.

References

1. Jiang, J.-Q.; Graham, N.; André, C.; Kelsall, G.H.; Brandon, N. Laboratory study of electro-coagulation–flotation for water treatment. *Water Res.* **2002**, *36*, 4064–4078. [[CrossRef](#)]
2. Lee, J.-B.; Park, K.-K.; Eum, H.-M.; Lee, C.-W. Desalination of a thermal power plant wastewater by membrane capacitive deionization. *Desalination* **2006**, *196*, 125–134. [[CrossRef](#)]
3. Liao, Z.; Gu, Z.; Schulz, M.C.; Davis, J.R.; Baygents, J.C.; Farrell, J. Treatment of cooling tower blowdown water containing silica, calcium and magnesium by electrocoagulation. *Water Sci. Technol.* **2009**, *60*, 2345–2352. [[CrossRef](#)]

4. Liu, Z.; Li, N.; Yan, M.; Guo, R.; Liu, Z. The research progress of water treatment technology on recirculated cooling water. *IOP Conf. Ser. Earth Environ. Sci.* **2020**, *508*, 012041. [[CrossRef](#)]
5. Kirilina, A.V.; Suslov, S.Y.; Kozlovskii, V.V.; Larin, A.B. Water Chemistry Development for a Thermal Power Plant Circulating Cooling System Using the VTIAMIN EKO-1 Chemical Agent. *Therm. Eng.* **2019**, *66*, 750–759. [[CrossRef](#)]
6. Wang, J.; Qu, D.; Tie, M.; Ren, H.; Peng, X.; Luan, Z. Effect of coagulation pretreatment on membrane distillation process for desalination of recirculating cooling water. *Sep. Purif. Technol.* **2008**, *64*, 108–115. [[CrossRef](#)]
7. Tang, C.; Zhang, C.; He, D.; Zhang, F.; Wei, Y.; Yang, Z.; Yan, Y. Research on Gravity Energy Saving Reconstruction Technology of Circulating Cooling Water in Mechanical Ventilation Cooling Tower of a Steel Plant. *Energies* **2023**, *16*, 6274. [[CrossRef](#)]
8. Chatterjee, A.; Huang, H.; Davis, K.R.; Layton, A. A Multigraph Modeling Approach to Enable Ecological Network Analysis of Cyber Physical Power Networks. In Proceedings of the 2021 IEEE International Conference on Communications, Control, and Computing Technologies for Smart Grids (SmartGridComm), Aachen, Germany, 25–28 October 2021; pp. 239–244.
9. Xu, J.; Zhao, J.; Jia, Y. Experimental study on the scale inhibition effect of the alternating electromagnetic field on CaCO₃ fouling on the heat exchanger surface in different circulating cooling water conditions. *Int. J. Therm. Sci.* **2023**, *192*, 108388. [[CrossRef](#)]
10. Tijng, L.D.; Yu, M.-H.; Kim, C.-H.; Amarjargal, A.; Lee, Y.C.; Lee, D.-H.; Kim, D.-W.; Kim, C.S. Mitigation of scaling in heat exchangers by physical water treatment using zinc and tourmaline. *Appl. Therm. Eng.* **2011**, *31*, 2025–2031. [[CrossRef](#)]
11. AzadiAghdam, M.; Park, M.; Lopez-Prieto, I.J.; Achilli, A.; Snyder, S.A.; Farrell, J. Pretreatment for water reuse using fluidized bed crystallization. *J. Water Process Eng.* **2020**, *35*, 101226. [[CrossRef](#)]
12. Choi, D.-J.; You, S.-J.; Kim, J.-G. Development of an environmentally safe corrosion, scale, and microorganism inhibitor for open recirculating cooling systems. *Mater. Sci. Eng. A* **2002**, *335*, 228–235. [[CrossRef](#)]
13. Rahmani, K.; Jadidian, R.; Haghtalab, S. Evaluation of inhibitors and biocides on the corrosion, scaling and biofouling control of carbon steel and copper–nickel alloys in a power plant cooling water system. *Desalination* **2016**, *393*, 174–185. [[CrossRef](#)]
14. Seo, S.-J.; Jeon, H.; Lee, J.K.; Kim, G.-Y.; Park, D.; Nojima, H.; Lee, J.; Moon, S.-H. Investigation on removal of hardness ions by capacitive deionization (CDI) for water softening applications. *Water Res.* **2010**, *44*, 2267–2275. [[CrossRef](#)]
15. Zhang, Z.; Jia, Y.; Zhao, J. Effect of Magnesium Ion Concentration on the Scale Inhibition of Heat Exchanger in Circulating Cooling Water under Alternating Electric Field. *Appl. Sci.* **2020**, *10*, 5491. [[CrossRef](#)]
16. Chaussemier, M.; Pourmohtasham, E.; Gelus, D.; Pécou, N.; Perrot, H.; Lédion, J.; Cheap-Charpentier, H.; Horner, O. State of art of natural inhibitors of calcium carbonate scaling. A review article. *Desalination* **2015**, *356*, 47–55. [[CrossRef](#)]
17. Han, Y.; Zhang, C.; Zhu, L.; Gao, Q.; Wu, L.; Zhang, Q.; Zhao, R. Effect of alternating electromagnetic field and ultrasonic on CaCO₃ scale inhibitive performance of EDTMPS. *J. Taiwan Inst. Chem. Eng.* **2019**, *99*, 104–112. [[CrossRef](#)]
18. Xu, J.; Zhao, J.-D.; Jia, Y.; Li, T.; Yang, S.-B.; Zhang, Z.-H. Effect of fouling resistance in heat exchanger and the crystal form of CaCO₃ in hard circulating cooling water with electrostatic field and alternating current electric field. *Water Sci. Technol.* **2021**, *84*, 1608–1622. [[CrossRef](#)] [[PubMed](#)]
19. Hu, Y.; Xu, Y.; Xie, M.; Huang, M.; Chen, G. Characterization of scalants and strategies for scaling mitigation in membrane distillation of alkaline concentrated circulating cooling water. *Desalination* **2022**, *527*, 115534. [[CrossRef](#)]
20. Zhang, Y.; Duan, H.; Chen, E.; Li, M.; Liu, S. Physicochemical Characteristics and the Scale Inhibition Effect of Air Nanobubbles (A-NBs) in a Circulating Cooling Water System. *Langmuir* **2023**, *39*, 1629–1639. [[CrossRef](#)] [[PubMed](#)]
21. Zhu, H.; Zheng, F.; Lu, S.; Hao, L.; Li, B.; Mao, Z.; Long, Y.; Yao, C.; Wu, H.; Zheng, X.; et al. Effect of electrochemical pretreatment on the control of scaling and fouling caused by circulating cooling water on heat exchanger and side-stream reverse osmosis membrane. *J. Water Process Eng.* **2021**, *43*, 102261. [[CrossRef](#)]
22. Bogart, S.J.; Woodman, S.; Steinkey, D.; Meays, C.; Pyle, G.G. Rapid changes in water hardness and alkalinity: Calcite formation is lethal to *Daphnia magna*. *Sci. Total Environ.* **2016**, *559*, 182–191. [[CrossRef](#)] [[PubMed](#)]
23. Vera, M.L.; Palacios, C.J.O.; Díaz Nieto, C.H.; Palacios, N.A.; Di Carantonio, N.; Luna, F.G.; Torres, W.R.; Flexer, V. A strategy to avoid solid formation within the reactor during magnesium and calcium electrolytic removal from lithium-rich brines. *J. Solid State Electrochem.* **2022**, *26*, 1981–1994. [[CrossRef](#)]
24. Gongye, F.; Zhou, J.; Peng, J.; Zhang, H.; Peng, S.; Li, S.; Deng, H. Study on the Removal of Oxide Scale Formed on 300 M Steel Special-Shaped Hot Forging Surfaces during Heating at Elevated Temperature by a High-Pressure Water Descaling Process. *Materials* **2023**, *16*, 1745. [[CrossRef](#)] [[PubMed](#)]
25. Xu, H.; Xu, Z.; Guo, Y.; Guo, S.; Xu, X.; Gao, X.; Wang, L.; Yan, W. Research and application progress of electrochemical water quality stabilization technology for recirculating cooling water in China: A short review. *J. Water Process Eng.* **2020**, *37*, 101433. [[CrossRef](#)]
26. Al-Hamzah, A.A.; Fellows, C.M. A comparative study of novel scale inhibitors with commercial scale inhibitors used in seawater desalination. *Desalination* **2015**, *359*, 22–25. [[CrossRef](#)]
27. Wang, Y.; Niu, X.; Xing, X.; Wang, S.; Jing, X. Curing behaviour and properties of a novel benzoxazine resin via catalysis of 2-phenyl-1,3,2-benzodioxaborole. *React. Funct. Polym.* **2017**, *117*, 60–69. [[CrossRef](#)]
28. Lin, Y.-P.; Singer, P.C. Inhibition of calcite crystal growth by polyphosphates. *Water Res.* **2005**, *39*, 4835–4843. [[CrossRef](#)]
29. Zhu, T.; Wang, L.; Sun, W.; Yang, Z.; Wang, S.; Zhou, Y.; He, S.; Wang, Y.; Liu, G. Corrosion-Induced Performance Degradation of Phosphorus-Containing Scale Inhibitors at Carbon Steel–Water Interface. *Ind. Eng. Chem. Res.* **2018**, *57*, 5183–5189. [[CrossRef](#)]
30. Ansari, S.Z.; Pandit, A.B. Optimising hydrodynamic conditions for inhibiting scale deposition on metal surfaces in the presence of aspartic acid. *Indian Chem. Eng.* **2022**, *64*, 337–347. [[CrossRef](#)]

31. Wang, Y.; Kuntke, P.; Saakes, M.; van der Weijden, R.D.; Buisman, C.J.N.; Lei, Y. Electrochemically mediated precipitation of phosphate minerals for phosphorus removal and recovery: Progress and perspective. *Water Res.* **2022**, *209*, 117891. [[CrossRef](#)]
32. Lei, Y.; Saakes, M.; van der Weijden, R.D.; Buisman, C.J.N. Electrochemically mediated calcium phosphate precipitation from phosphonates: Implications on phosphorus recovery from non-orthophosphate. *Water Res.* **2020**, *169*, 115206. [[CrossRef](#)]
33. Wang, Q.; Lenhart, J.J.; Walker, H.W. Recovery of metal cations from lime softening sludge using Donnan dialysis. *J. Membr. Sci.* **2010**, *360*, 469–475. [[CrossRef](#)]
34. Kausley, S.B.; Desai, K.S.; Patil, R.A.; Malhotra, C.P.; Pandit, A.B. Comparative study of lime softening, soda ash process, and electrocoagulation for the removal of hardness from groundwater. *Proc. Indian Natl. Sci. Acad.* **2022**, *88*, 379–391. [[CrossRef](#)]
35. Zhao, K.; Wu, J.; Li, X.; Li, Z.; Chen, Y. Advances of Ultrasonic Scaling Removal Technology and Heat Transfer Enhancement Technology. *ChemBioEng Rev.* **2021**, *8*, 134–144. [[CrossRef](#)]
36. Karabelas, A.J.; Mitrouli, S.T.; Kostoglou, M. Scaling in reverse osmosis desalination plants: A perspective focusing on development of comprehensive simulation tools. *Desalination* **2020**, *474*, 114193. [[CrossRef](#)]
37. Cinperi, N.C.; Ozturk, E.; Yigit, N.O.; Kitis, M. Treatment of woolen textile wastewater using membrane bioreactor, nanofiltration and reverse osmosis for reuse in production processes. *J. Clean. Prod.* **2019**, *223*, 837–848. [[CrossRef](#)]
38. Altmann, T.; Das, R. Process improvement of sea water reverse osmosis (SWRO) and subsequent decarbonization. *Desalination* **2021**, *499*, 114791. [[CrossRef](#)]
39. Wang, X.-X.; Wu, Y.-H.; Zhang, T.-Y.; Xu, X.-Q.; Dao, G.-H.; Hu, H.-Y. Simultaneous nitrogen, phosphorous, and hardness removal from reverse osmosis concentrate by microalgae cultivation. *Water Res.* **2016**, *94*, 215–224. [[CrossRef](#)] [[PubMed](#)]
40. Kim, J.; Hong, S. A novel single-pass reverse osmosis configuration for high-purity water production and low energy consumption in seawater desalination. *Desalination* **2018**, *429*, 142–154. [[CrossRef](#)]
41. Guo, Y.; Xu, Z.; Guo, S.; Chen, S.; Xu, H.; Xu, X.; Gao, X.; Yan, W. Selection of anode materials and optimization of operating parameters for electrochemical water descaling. *Sep. Purif. Technol.* **2021**, *261*, 118304. [[CrossRef](#)]
42. Ba, X.; Chen, J.; Wang, X.; Xu, H.; Sun, J.; Qi, Y.; Li, Y.; Wang, J.; Jiang, B. An integrated electrolysis-microfiltration-ion exchange closed-loop system for effective water softening without chemicals input and spent regenerant discharge. *Desalination* **2023**, *553*, 116481. [[CrossRef](#)]
43. Sanjuán, I.; Benavente, D.; García-García, V.; Expósito, E.; Montiel, V. Electrochemical softening of concentrates from an electrodialysis brackish water desalination plant: Efficiency enhancement using a three-dimensional cathode. *Sep. Purif. Technol.* **2019**, *208*, 217–226. [[CrossRef](#)]
44. Clauwaert, P.; De Paepe, J.; Jiang, F.; Alonso-Fariñas, B.; Vaiopoulou, E.; Verliefde, A.; Rabaey, K. Electrochemical tap water softening: A zero chemical input approach. *Water Res.* **2020**, *169*, 115263. [[CrossRef](#)] [[PubMed](#)]
45. Hasson, D.; Sidorenko, G.; Semiat, R. Calcium carbonate hardness removal by a novel electrochemical seeds system. *Desalination* **2010**, *263*, 285–289. [[CrossRef](#)]
46. Tlili, M.M.; Benamor, M.; Gabrielli, C.; Perrot, H.; Tribollet, B. Influence of the interfacial pH on electrochemical CaCO₃ precipitation. *J. Electrochem. Soc.* **2003**, *150*, C765–C771. [[CrossRef](#)]
47. Liu, Y.; Wu, J.; Chen, J.; Liu, S.; Xu, H.; Yang, Q.; Xu, F.; Guo, Y.; Jiang, B. Robust electrolysis system divided by bipolar electrode and non-conductive membrane for energy-efficient calcium hardness removal. *Chemosphere* **2023**, *331*, 138797. [[CrossRef](#)]
48. Sanjuán, I.; Benavente, D.; Expósito, E.; Montiel, V. Electrochemical water softening: Influence of water composition on the precipitation behaviour. *Sep. Purif. Technol.* **2019**, *211*, 857–865. [[CrossRef](#)]
49. Zeppenfeld, K. Electrochemical water softening: The role of alkalinity. *Water Solut.* **2019**, *4*, 28–31.
50. Wang, Z.; Lin, W.; Wang, W.; Wang, Z.; Li, J.; Xu, J.; Yu, J. Research on performance optimization and mechanism of electrochemical water softening applied by pulse power supply. *Water Sci. Technol.* **2021**, *84*, 2432–2445. [[CrossRef](#)] [[PubMed](#)]
51. Yin, F.; Liu, H. The j–pH diagram of interfacial reactions involving H⁺ and OH[−]. *J. Energy Chem.* **2020**, *50*, 339–343. [[CrossRef](#)]
52. Zhou, J.; Liu, J.; Rao, Y.; Yang, L.; Jiang, B.; Yan, W.; Xu, X.; Xu, H. Application of titanium suboxide electrode in electrochemical polarity reversal descaling-filtration crystallization coupling system. *Desalination* **2023**, *568*, 117028. [[CrossRef](#)]
53. Jin, H.; Yu, Y.; Chen, X. Membrane-based electrochemical precipitation for water softening. *J. Membr. Sci.* **2020**, *597*, 117639. [[CrossRef](#)]
54. Zaslavski, I.; Shemer, H.; Hasson, D.; Semiat, R. Electrochemical CaCO₃ scale removal with a bipolar membrane system. *J. Membr. Sci.* **2013**, *445*, 88–95. [[CrossRef](#)]
55. Liu, Y.; Niu, Q.; Zhu, J.; Li, Y.; Sun, H.; Jiang, B. Efficient and green water softening by integrating electrochemically accelerated precipitation and microfiltration with membrane cleaning by periodically anodic polarization. *Chem. Eng. J.* **2022**, *449*, 137832. [[CrossRef](#)]
56. Li, Y.; Wang, L.; Wang, L. Facilitating removal efficiency of electrochemical descaling system using confined crystallization membranes. *J. Water Process Eng.* **2023**, *56*, 104338. [[CrossRef](#)]
57. Ba, X.; Chen, J.; Wang, X.; Feng, F.; Shi, X.; Qi, Y.; Wang, J.; Jiang, B. Anode Boundary Layer Extraction Strategy for H⁺–OH[−] Separation in Undivided Electrolytic Cell: Modeling, Electrochemical Analysis, and Water Softening Application. *ACS ES&T Eng.* **2023**, *3*, 2183–2193.
58. Kang, W.; Li, L.; Yan, L.; Mao, W.; Wang, X.; Yu, H.; Ma, C. Spatial and temporal regulation of homogeneous nucleation and crystal growth for high-flux electrochemical water softening. *Water Res.* **2023**, *232*, 119694. [[CrossRef](#)] [[PubMed](#)]

59. Mao, W.; Gu, Y.; Kang, W.; Yu, H. Facilitated OH⁻ diffusion via bubble motion and water flow in a novel electrochemical reactor for enhancing homogeneous nucleation of CaCO₃. *Water Res.* **2023**, *242*, 120195. [[CrossRef](#)] [[PubMed](#)]
60. Comstock, S.E.H.; Boyer, T.H. Combined magnetic ion exchange and cation exchange for removal of DOC and hardness. *Chem. Eng. J.* **2014**, *241*, 366–375. [[CrossRef](#)]
61. Feng, S.; Zhong, Z.; Wang, Y.; Xing, W.; Drioli, E. Progress and perspectives in PTFE membrane: Preparation, modification, and applications. *J. Membr. Sci.* **2018**, *549*, 332–349. [[CrossRef](#)]
62. Zhang, C.; Tang, J.; Zhao, G.; Tang, Y.; Li, J.; Li, F.; Zhuang, H.; Chen, J.; Lin, H.; Zhang, Y. Investigation on an electrochemical pilot equipment for water softening with an automatic descaling system: Parameter optimization and energy consumption analysis. *J. Clean. Prod.* **2020**, *276*, 123178. [[CrossRef](#)]
63. Huang, L.; Li, D.; Liu, J.; Yang, L.; Dai, C.; Ren, N.; Feng, Y. CFD simulation of mass transfer in electrochemical reactor with mesh cathode for higher phenol degradation. *Chemosphere* **2021**, *262*, 127626. [[CrossRef](#)]
64. Lin, W.; Wang, Z.; Wang, W.; Chen, Q.; Xu, J.; Yu, J. Comparative analysis the performance of electrochemical water softening between high frequency electric fields and direct current electric fields based on orthogonal experimental methods. *Water Sci. Technol.* **2021**, *83*, 1677–1690. [[CrossRef](#)] [[PubMed](#)]
65. Chen, L.; Alshawabkeh, A.N.; Hojabri, S.; Sun, M.; Xu, G.; Li, J. A Robust Flow-Through Platform for Organic Contaminant Removal. *Cell Rep. Phys. Sci.* **2021**, *2*, 100296. [[CrossRef](#)] [[PubMed](#)]
66. Meng, X.; Li, K.; Zhao, Z.; Li, Y.; Yang, Q.; Jiang, B. A pH self-regulated three-dimensional electro-Fenton system with a bifunctional Fe-Cu-C particle electrode: High degradation performance, wide working pH and good anti-scaling ability. *Sep. Purif. Technol.* **2022**, *298*, 121672. [[CrossRef](#)]
67. Chen, Y.; Shen, M.; Chen, Y.; Zou, Y.; Gong, Y. Study on electrolytic bubble size and its distribution by means of laser diffraction method. *Acta Chim. Sinica* **1992**, *50*, 967–972.
68. Emmel, B.U.; Gawel, K.M.; Bhuiyan, M.H.; Torsæter, M.; Edvardsen, L. Electrochemically Enhanced Deposition of Scale from Chosen Formation Waters from the Norwegian Continental Shelf. *Energies* **2022**, *15*, 542. [[CrossRef](#)]
69. Gabrielli, C.; Maurin, G.; Francy-Chausson, H.; Thery, P.; Tran, T.T.M.; Tlili, M. Electrochemical water softening: Principle and application. *Desalination* **2006**, *201*, 150–163. [[CrossRef](#)]
70. Gao, J.; Shi, N.; Guo, X.; Li, Y.; Bi, X.; Qi, Y.; Guan, J.; Jiang, B. Electrochemically Selective Ammonia Extraction from Nitrate by Coupling Electron- and Phase-Transfer Reactions at a Three-Phase Interface. *Environ. Sci. Technol.* **2021**, *55*, 10684–10694. [[CrossRef](#)]
71. Hasson, D.; Lumelsky, V.; Greenberg, G.; Pinhas, Y.; Semiat, R. Development of the electrochemical scale removal technique for desalination applications. *Desalination* **2008**, *230*, 329–342. [[CrossRef](#)]
72. Luan, J.; Wang, L.; Sun, W.; Li, X.; Zhu, T.; Zhou, Y.; Deng, H.; Chen, S.; He, S.; Liu, G. Multi-meshes coupled cathodes enhanced performance of electrochemical water softening system. *Sep. Purif. Technol.* **2019**, *217*, 128–136. [[CrossRef](#)]
73. Yu, Y.; Jin, H.; Quan, X.; Hong, B.; Chen, X. Continuous Multistage Electrochemical Precipitation Reactor for Water Softening. *Ind. Eng. Chem. Res.* **2019**, *58*, 461–468. [[CrossRef](#)]
74. Marchesiello, M.; Thivel, P.X. Electrochemical antiscaling treatment using a fluidized bed. *Sep. Purif. Technol.* **2018**, *194*, 480–487. [[CrossRef](#)]
75. Yang, Q.; Xu, L.; He, Q.; Wu, D. Reduced cathodic scale and enhanced electrochemical precipitation of Ca²⁺ and Mg²⁺ by a novel fenced cathode structure: Formation of strong alkaline microenvironment and favorable crystallization. *Water Res.* **2022**, *209*, 117893. [[CrossRef](#)]
76. Muddemann, T.; Haupt, D.; Engelke, M.; Sievers, M.; Fischer, A.; Kiefer, C.; Filip, K.; Zielinski, O.; Hickmann, T.; Kunz, U. Combination of magnetically actuated flexible graphite–polymer composite cathode and boron-doped diamond anode for electrochemical water softening or wastewater treatment. *Electrochim. Acta* **2020**, *354*, 136729. [[CrossRef](#)]
77. Yu, Y.; Jin, H.; Meng, P.; Guan, Y.; Shao, S.; Chen, X. Electrochemical water softening using air-scoured washing for scale detachment. *Sep. Purif. Technol.* **2018**, *191*, 216–224. [[CrossRef](#)]
78. Li, X.; Wang, L.; Sun, W.; Yan, Z.; He, Y.; Shu, X.; Liu, G. Study on electrochemical water softening mechanism of high-efficient multi-layer mesh coupled cathode. *Sep. Purif. Technol.* **2020**, *247*, 117001. [[CrossRef](#)]
79. Jiang, B.; Ren, X.; Liu, Q.; Yue, X.; Yang, Q.; Liu, Y.; Xu, H.; Zhou, J. Electrochemical water softening technology: From fundamental research to practical application. *Water Res.* **2024**, *250*, 121077. [[CrossRef](#)] [[PubMed](#)]
80. Mahasti, N.N.N.; Shih, Y.-J.; Vu, X.-T.; Huang, Y.H. Removal of calcium hardness from solution by fluidized-bed homogeneous crystallization (FBHC) process. *J. Taiwan Inst. Chem. Eng.* **2017**, *78*, 378–385. [[CrossRef](#)]
81. Tiangco, K.A.A.; de Luna, M.D.G.; Vilando, A.C.; Lu, M.-C. Removal and recovery of calcium from aqueous solutions by fluidized-bed homogeneous crystallization. *Process Saf. Environ. Prot.* **2019**, *128*, 307–315. [[CrossRef](#)]
82. Jiang, B.; Ren, X.; Liu, Q.; Yue, X.; Yang, Q.; Liu, Y.; Xu, H.; Zhou, J. A critical review on the electrochemical water softening technology from fundamental research to practical application. *Water Res.* **2023**, *250*, 121077. [[CrossRef](#)]
83. Zhi, S.; Zhang, K. Hardness removal by a novel electrochemical method. *Desalination* **2016**, *381*, 8–14. [[CrossRef](#)]
84. Yu, Y.; Zhang, M.; Li, Q.; Chen, X.; Chen, D.; Jin, H. Subtle introduction of membrane polarization-catalyzed H₂O dissociation actuates highly efficient electrocoagulation for hardness ion removal. *Water Res.* **2023**, *242*, 120240. [[CrossRef](#)] [[PubMed](#)]

85. Yifei, G.; Zhicheng, X.; Siyuan, G.; Jianyi, L.; Hao, X.; Xing, X.; Xian, G.; Wei, Y. Practical optimization of scale removal in circulating cooling water: Electrochemical descaling-filtration crystallization coupled system. *Sep. Purif. Technol.* **2022**, *284*, 120268. [[CrossRef](#)]
86. Yu, Y.; Chen, D.; Liu, H.; Zhang, X.; Chen, X.; Jin, H. Membrane deposition electro dialysis for cooling water treatment: Ion step removal and stable membrane regeneration. *Chem. Eng. J.* **2023**, *451*, 138908. [[CrossRef](#)]
87. Medina-Collana, J.T.; Reyna-Mendoza, G.E.; Montaña-Pisfil, J.A.; Rosales-Huamani, J.A.; Franco-Gonzales, E.J.; Córdova García, X. Evaluation of the Performance of the Electrocoagulation Process for the Removal of Water Hardness. *Sustainability* **2023**, *15*, 590. [[CrossRef](#)]
88. Choi, J.; Dorji, P.; Shon, H.K.; Hong, S. Applications of capacitive deionization: Desalination, softening, selective removal, and energy efficiency. *Desalination* **2019**, *449*, 118–130. [[CrossRef](#)]
89. Karabacakoglu, B.; Tezakıl, F.; Güvenç, A. Removal of hardness by electro dialysis using homogeneous and heterogeneous ion exchange membranes. *Desalination Water Treat.* **2015**, *54*, 8–14. [[CrossRef](#)]
90. Panagopoulos, A. Energetic, economic and environmental assessment of zero liquid discharge (ZLD) brackish water and seawater desalination systems. *Energy Convers. Manag.* **2021**, *235*, 113957. [[CrossRef](#)]

Disclaimer/Publisher’s Note: The statements, opinions and data contained in all publications are solely those of the individual author(s) and contributor(s) and not of MDPI and/or the editor(s). MDPI and/or the editor(s) disclaim responsibility for any injury to people or property resulting from any ideas, methods, instructions or products referred to in the content.